DR. 742

DSE-23047-T1

THIN FILM POLYCRYSTALLINE SILICON SOLAR CELLS

Quarterly Report No. 1, January 1—March 31, 1979

By
Amal K. Ghosh
Tom Feng
H. Paul Maruska
Charles Fishman

Work Performed Under Contract No. AC02-79ET23047

Exxon Research and Engineering Company
Linden, New Jersey

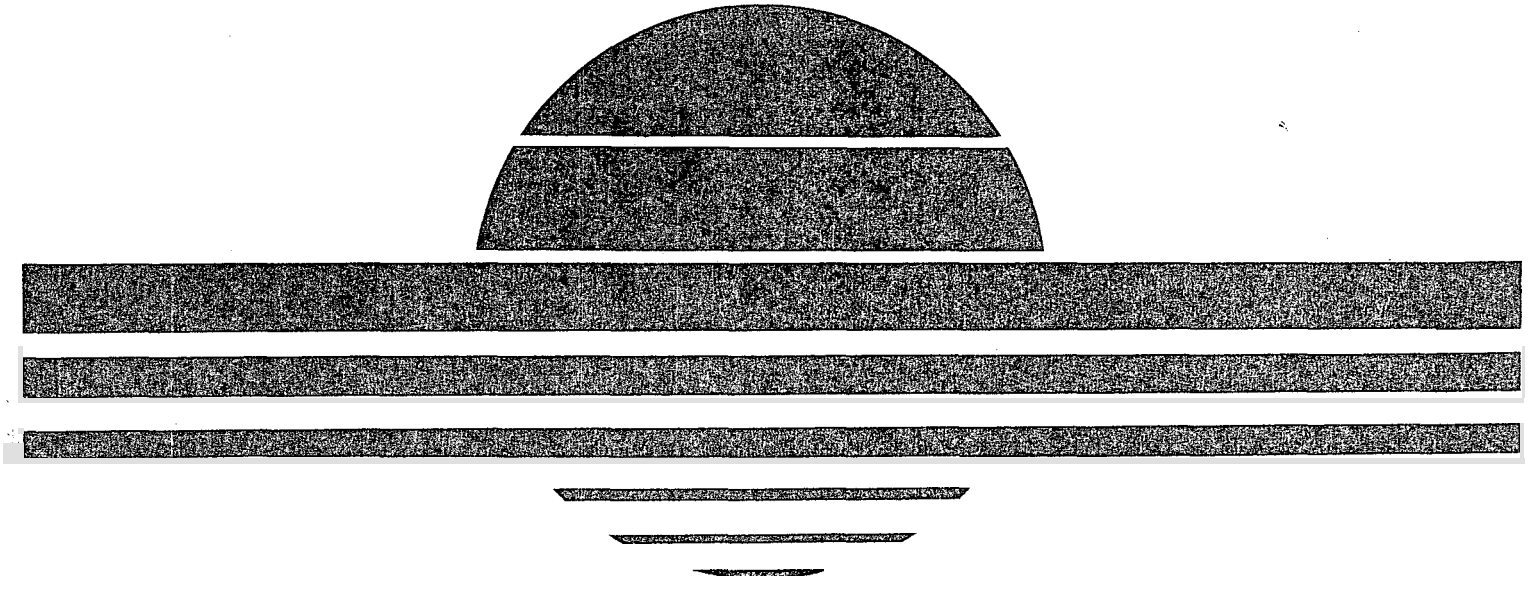

U.S. Department of Energy

Solar Energy

NOTICE

DSE-23047-T1
Distribution Category UC-63e

CORPORATE APPLIED RESEARCH

EXXON RESEARCH AND ENGINEERING COMPANY • LINDEN, NEW JERSEY

THIN FILM POLYCRYSTALLINE SILICON SOLAR CELLS

Quarterly Report #1
Period: January 1, 1979 - March 31, 1979

950 1053

Contract No. DE-AC03-79ET23047

By

Amal K. Ghosh
Tom Feng
H. Paul Maruska
Charles Fishman

This work was performed for
U.S. Department of Energy,
under Contract No. DE-AC02-79ET23047

DISCLAIMER

PREFACE

This is the first quarterly report. During this quarter we have made great progress in the area of modelling, while initiating fabrication and characterization studies of Heterostructure, MIS and diffused polycrystalline silicon solar cells. The present report details our work on modelling. Reports on other areas will be forthcoming in the future.

AIM OF PROJECT

The aim of the project is to model, fabricate and characterize heterostructure, p/n junction and MIS polycrystalline silicon solar cells, with a view toward evaluating the best fabrication process for low cost cells.

TABLE OF CONTENTS

ABSTRACT

A theory capable of predicting the performance of polycrystalline silicon solar cells is formulated. It relates grain size to mobility, lifetime, diffusion length, reverse saturation current, open circuit photovoltage and fill factor. Only the diffusion lengths measured by the surface photovoltage technique for grains $\lesssim 5$ μm do not agree with our theory. The reason for this discrepancy is presently being investigated. We conclude that grains $\geq$ 100μm are necessary to achieve efficiencies $\geq$ 10 percent at AM1 irradiance. The calculations were performed for the case of no grain boundary passivation. At present we are investigating the improvements to be expected from grain boundary passivation.

We have determined that the parameters that best fit the available data are as follows:

1. Number of surface states at grain boundaries acting as recombination centers - $1.6 \times 10^{13}/cm^2$
2. Capture cross section - 2×10^{-16} cm^2
3. Surface recombination velocity at grain boundary - 3.2×10^4 cm/sec.

The following types of solar cells are considered in the model: SnO_2/Si Heterostructure, MIS, and p/n junction. In all types of solar cells considered, grain boundary recombination plays a dominant role, especially for small grains. Though the calculations were originally expected to yield only order of magnitude results, they have proven to be accurate for most parameters within 10 percent.

It is almost impossible to cover every aspect of solar cell performance in one theory. But we feel that the present theory is the most extensive theory ever postulated for polycrystalline silicon solar cells. In the future, as more data becomes available, we will try to refine and modify the theory.

As a result of the theory we are capable of directing an experimental effort in a more logical fashion. The data base of the theory involves almost all the DOE funded projects, and more. The theory provides a basis to judge the status and capabilities of the different polycrystalline efforts.

2. THEORY OF POLYCRYSTALLINE SILICON SOLAR CELL

I. INTRODUCTION

The potential of polycrystalline silicon for large scale terrestrial photovoltaic device application is well recognized. It shares with single crystal silicon numerous desirable physical and chemical properties such as abundance, low toxicity, and stability, while also showing great promise of reduced costs by circumventing many of the complex and energy intensive steps associated with the growth of single crystals. These facts have prompted many scientists to investigate various forms and shapes of polycrystalline silicon, with the principal objective of approaching the efficiencies obtained with single crystal silicon ($\geq$ 10%) while minimizing the cost of the material. Several experimental[1-13] and theoretical[14-17] results have indicated that there is an increase in the efficiency of polycrystalline silicon solar cells with increasing grain sizes, and some of these results are shown in Fig. 1. The theoretical results are based on a variety of assumptions, and the experimental results are for devices prepared under widely different conditions. There exists a gap between theory and experiment which the present paper attempts to fill. Our formulation will allow for the first time that polycrystalline silicon prepared under different conditions can be compared on the same basis. It will be shown that the differences in the photovoltaic properties of materials deposited under widely varying conditions can be understood in terms of grain size effects.

Fig. 2 shows a solar cell with grain boundaries at different physical locations. Type 1 grain boundaries are associated with columnar growth, Type 2 grain boundaries are in the bulk of the crystal, and Type 3 grain boundaries are in the barrier region. Most theoretical calculations[14-17] have been made for the short-circuit photocurrent of columnar-growth polycrystalline solar cells. The open circuit photovoltages and fill factors were

were assumed to be the same as in single crystals. In our theory, all three types of grain boundaries will be taken into account, and the efficiency will be calculated after estimating the effects of grain boundary states on short-circuit photocurrent, open-circuit photovoltage and the fill factor. It will be shown that the results of measurements on solar cell type devices indicate that grain boundary states not only act as traps but also as efficient recombination centers having capture cross sections of about 2×10^{-16} cm^2 and giving rise to surface recombination velocities of $\approx 3 \times 10^4$ cm/sec. It will be shown that this theory can best account for the various results observed for polycrystalline silicon solar cells.

II. THEORY

A. Effect of Grain Size on Free Carrier Concentration, Mobility, and Resistivity

The resistivity, mobility and free carrier concentration of polycrystalline silicon do not vary with doping concentration in the same manner as has been observed for single crystal silicon [18-25] The impurity concentration and the free carrier concentration are in general not identical in polycrystalline silicon. It is well known that doping plays an important role in the performance of solar cells and cannot be ignored. In Fig. 3 the variation of the majority carrier mobility, and free carrier density as a function of doping density is shown for two grain sizes. The dopant concentration at which the mobility minimum and the sharp increase in free majority carrier concentration occurs follows roughly the relation

$$N_d \sim 10^{12}/d \qquad (1)$$

where d is the grain size in cm and N_d is the doping density. The variation of N_d with d is shown in Fig. 4. The constant $10^{12}/cm^2$ is possibly related to traps at grain boundaries.[18] Three different studies[18,21,22] indicate

the order of magnitude of grain boundary traps within $\pm$ 0.02 eV of the mid gap to be ~$10^{12}/cm^2$. Whether these traps act as recombination centers is not known.

In Fig. 5, the resistivities of polycrystalline films are compared to those of single crystal silicon for different dopant concentrations.[18,25] In designing solar cells with polysilicon, it is preferable to be on the higher doping density side of the minimum. As will be shown later, for grain sizes below 100 μm the change of lifetime as a function of doping is not as severe as the effects of surface recombination velocity. Surprisingly, most of the experimental data on polycrystalline solar cells are for dopant densities which are higher than the predicted density at which the mobility minimum occurs. In Fig. 6 the available experimental values of majority carrier mobility as a function of grain sizes are shown both for electrons and holes. (For 1 cm grain size the single crystal value has been assigned.) We shall assume that the minority carriers have the same mobility as the majority carriers, and justify this assignment subsequently. In one calculation, as shown in Fig. 6, we have assumed that the minority carrier mobility for grain sizes greater than 100 μm is 500 cm^2/volt-sec., while for grains less than 10 μm the value is about 80 cm^2/volt-sec. The effect of decreasing mobility as the grain size decreases is actually small relative to the effect of decreasing lifetime. Card and Yang[17] in their theory of polycrystalline silicon have actually neglected any change in mobility as a function of grain size. They have postulated that the change in lifetime is the more dominant factor in determining solar cell parameters, and we agree with this part of the assumption. So, if we assume either a linear variation or no variation of mobility, the effect on our calculation of short circuit photocurrent will be small, especially since there is only a square root dependence on mobility.

B. Effect of Grain Size on Lifetime

The carrier lifetime for small grains can be different from that of single crystals, a fact long recognized. The effective lifetime of granular semiconductors has two components[26] τ_b and τ_s for volume and surface lifetimes, respectively,and given by Eq. (2)

$$\frac{1}{\tau_{eff}} = \frac{1}{\tau_b} + \frac{1}{\tau_s} . \tag{2}$$

For small grain sizes $\tau_s << \tau_b$, and τ_s dominates the effective lifetime.

Shockley[26] derived equations relating τ_s and the cross sectional dimensions for a rectangular filament of cross section 2B x 2C. He showed

$$\frac{1}{\tau_s} = \frac{\pi^2 D}{4} \left(\frac{1}{B^2} + \frac{1}{C^2}\right), \text{ for } s \to \infty \tag{3}$$

and

$$\frac{1}{\tau_s} = s \left(\frac{1}{B} + \frac{1}{C}\right), \text{ for } s \to o \tag{4}$$

where s is the surface recombination velocity and D is the diffusivity. Loferski[27] has extended Shockley's calculations to include cylindrical filaments and found

$$\frac{1}{\tau_s} = \frac{D\pi}{2R^2}, \text{ for } s \to \infty \tag{5}$$

where R is the radius of the cylinder. For τ_{eff} or τ_s to be 10^{-5} sec, he estimated that R should be 130 μm. Recently Card and Yang[17] have derived an expression for the effective lifetime as

$$\tau_{eff} = \frac{2d \exp(-qV_d/kT)}{3\sigma v N_{is}(E_{fn}-E_{fp})} \tag{6}$$

Here N_{is} is the interface density (cm^{-2} eV^{-1}), σ is the capture cross section, v is the thermal velocity of the carriers, V_d is the height of the diffusion potential at the grain boundaries, and E_{fn} and E_{fp} are the quasi-Fermi levels for electrons and holes, respectively. They assumed each grain is in the shape of a cube with dimension d, although Eq (6) should be applicable to other geometries. There are trapped charges at the grain boundaries, and the photogenerated minority carriers neutralize this charge, reducing the barrier height to such an extent that both types of photogenerated carriers can then penetrate the barrier region. Such carriers consequently encounter recombination centers at the boundary, and thus the effective minotrity carrier lifetime is reduced. In our calculations we find that it is actually possible to obtain a good estimate of the lifetime without considering the diffusion potential at the grain boundary. The following relation is sufficient to determine the effective minority carrier lifetime:

$$\tau_{eff} = \frac{1}{\sigma v N_{sr}}, \qquad (7)$$

where N_{sr} is the effective density of recombination centers (cm^{-3}). For mathematical convenience we are considering that the surface recombination sites can be treated as distributed uniformly throughout the bulk of the material. The number of these assumed effective sites in the bulk, N_{sr}, will therefore be portional to the actual fixed number of recombination sites at the surface. This transformation of a polycrystalline material with particular spatial location of recombination sites to a single crystal material with a uniform distribution of recombination centers provides a simple model that will be shown to be in excellent agreement with a variety of observations. This transformation is valid for small grains,

although for large grains the effective lifetime approaches the bulk lifetime for single crystal material.

If we assume cubic geometry for the crystallite, the number of recombination centers per unit volume is given by

$$N_{sr} = 6N_{ss}/d, \tag{8}$$

where N_{ss} is the concentration of recombination centers per unit area at the grain boundary. Except for a change in the value of the constant, the relation is quite general and holds for a wide variety of grain geometries varying from rectangular to cylindrical to spherical shapes. The effective lifetime based on the above transformation now becomes

$$\tau_{eff} = \frac{d}{6\sigma v N_{ss}}. \tag{9}$$

Assuming $\sigma = 2 \times 10^{-16} cm^2$ (the measured capture crossection for surface states) $v = 10^7$ cm/sec and $N_{ss} = 1.6 \times 10^{13}/cm^2$,

$$\tau_{eff} = 5 \times 10^{-6} d. \tag{10}$$

Our simple model will be shown to be capable of explaining all the observed parameters associated with polycrystalline silicon solar cells and of predicting the right directions one needs to follow to improve the efficiency of the cell. EPR studies indicate the number of paramagnetic centers to be in close agreement with our estimated value for N_{ss}.

The plot of τ_{eff} vs. d is shown in Fig. 7. It shows good agreement with the available experimental results, and appears to be independent of material preparation conditions. The hole lifetime for grains larger than 1 cm was assumed to be the same as the hole lifetime for single crystal silicon (1-10Ω-cm). The lifetime reported by Duh et al.[28] for CVD deposited polycrystalline silicon (grain size about 300 μm) was determined by open-circuit photovoltage decay. The lifetime for smaller grain sizes was determined mainly

from the recombination component of the reverse saturation current.[29,30] We assume the minority carrier lifetimes for electrons and holes are the same for polycrystalline silicon.

C. Effect of Grain Size on Diffusion Length

Having calculated the mobility and lifetime as a function of grain size, the diffusion length of the minority carriers can be determined as a function of grain size from the Einstein relation.

$$L = \left(\frac{\mu\tau kT}{q}\right)^{1/2} = 3.6 \times 10^{-4}(\mu d)^{1/2} \qquad (11)$$

and is plotted in Fig. 8. Experimental results are included for comparison.

The diffusion length of electrons for grain sizes below 10 μm was reported[9] to be determined by the surface photovoltage method. The plot of relative photon flux density vs. the inverse of the absorption constant did not give a straight line as it does for single crystal material. We believe that the experimental results are in error, because even without comparing with our theoretical plot, the results are not self-consistent. Though an increase in short-circuit photocurrent with an increase in grain size is observed, no correlation is observed between the measured diffusion length and short-circuit photocurrent. Even assuming the mobility to be 500 cm^2/volt-sec, the estimated diffusion length consistent with the measured short-circuit photocurrent is less than the experimental value. Later we will show that our theoretically estimated short-circuit photocurrent based on the theoretical diffusion lengths shown in Fig. 8 agrees very well with the reported experimental short-circuit photocurrent for the same grain size. The larger grain size values agree fairly well with experimental results.[31]

III. DEVICE PARAMETERS ASSOCIATED WITH POLYCRYSTALLINE SILICON SOLAR CELLS

Having derived relations indicating how mobility, lifetime, and diffusion length vary as a function of grain size, we are in a position to postulate a general theory of polycrystalline silicon solar cells. This theory will be valid for MIS type cells, SnO_2/Si or ITO/Si heterostructure cells[32-35], and p/n junction solar cells.[36]

A. The Dark I-V Characteristics

The dark I-V characteristics of any solar cell are usually given by the relation

$$J = J_{od}\,(e^{\lambda_d V}-1) + J_{ot}\,(e^{\lambda_t V}-1) + J_{or}(e^{\lambda_r V}-1) \qquad (12)$$

in which

$\lambda_d = q/n_d kT$, $\lambda_t = q/n_t kT$, $\lambda_r = q/n_r kT$

J_{od} = Reverse saturation current due to diffusion = $\frac{qD_p P_{no}}{L_p} + \frac{qD_n n_{po}}{L_n}$

and $n_d = 1$,

J_{ot} = Reverse saturation current due to thermonic emission for MIS or SnO_2/Si or ITO/Si cell = $AT^2\exp(-\phi_B/kT)$

and $n_t > 2$, and

J_{or} = Reverse saturation current due to recombination = $\frac{qn_i W}{2\tau}$

and $n_r = 2$.

The other symbols have their usual definitions.

For polycrystalline silicon of grain size 100 μm or less, the recombination component dominates over the thermionic term (barrier height $\geq$ 0.8ev); therefore, the thermionic term can be neglected. The general dark I-V curve is then given by the relation

$$J = J_{od}\,(e^{\lambda_d V} - 1) + J_{or}(e^{\lambda_r V} - 1). \tag{13}$$

Our calculations show that $J_{or} > J_{od}$ for grain sizes $\leq$ 100 μm as presented in Figure 9, and therefore we find that

$$J = J_{or}(e^{\lambda_r V} - 1) \tag{14}$$

for small grains.

On the other hand we have calculated that for grains sizes above a few hundred μm and at a forward bias near V_{oc}, the diffusion component becomes dominant, and there may also be some contribution from J_{ot}. The relation to be used for large grain sizes is therefore

$$J = J_{ot}\,(e^{\lambda_t V} - 1) + J_{od}\,(e^{\lambda_d V} - 1) \tag{15}$$

Fig. 9 shows a plot of J_{or} vs. d. Since $\tau = 5 \times 10^{-6}$ d, it follows that

$$J_{or} = \frac{q n_i W}{10^{-5} d}. \tag{16}$$

The experimental values[8,9] agree very well with our theoretical plot for grain sizes < 10 μm. The polysilicon in those experiments was electron beam deposited and the junctions were formed by diffusion. For many of the experimental J_{or} values, the analysis of the curves was done assuming infinite shunt

resistance and zero series resistance. The single crystal value was used for the cm size grain. J_{or} values in the range 10^{-5} to 10^{-7} are those reported by Chu and co-workers[37] for CVD silicon on recrystallized metallurgical silicon substrate.

B. The Short-Circuit Photocurrent

Since we have now found the values of mobility, lifetime, and diffusion length as functions of grain size, the short-circuit photocurrent can easily be calculated.

For MIS and SnO_2/Si or ITO/Si heterostructure devices[35] one can write

$$D_p \frac{d^2p}{dx^2} - \frac{p-p_o}{\tau} + \alpha_2 N^1 \exp(-\alpha_2 n) = 0. \tag{17}$$

Using the boundary conditions

$$p = p_o \exp(qV/kT) \text{ at } n = \ell_2 \text{ and } p = p_o \text{ at } n = d, \tag{18}$$

we can solve for the current J_2[35] from the bulk contribution and get

$$J_2 = q\left[\frac{\alpha_2 N^1 \exp(-\alpha_2 \ell_2)}{\alpha_2 + 1/L_p} - \frac{2\alpha_2 N^1 \exp(-\alpha_2 \ell_2)\,[\exp(-d/L_p) - \exp(-\alpha_2 d)]}{L_p(\alpha_2^2 - 1/L_p^2)\,[\exp(d/L_p) - \exp(-d/L_p)]}\right]. \tag{19}$$

The current from the barrier contribution is

$$J_1 = GqN^1[1 - \exp(-\alpha_2 \ell_2)]. \tag{20}$$

$$G = \tau/T \tag{21}$$

where τ is the lifetime and T is the transit time which can be expressed as

$$T = \frac{\ell_2^2}{V_d \mu}, \tag{22}$$

in which ℓ_2 is the width of the barrier region and V_d is built-in potential. If $\tau \geq T$, then G = 1. For the case $\tau < T$, G is less than 1, and not all carriers generated within the barrier are collected.

The total current for SnO_2/Si or ITO/Si heterostructure or MIS devices is

$$J_{sc} = J_2 + J_1. \tag{23}$$

The definitions of the symbols used in these equations are given in reference 35.

For p/n junction cells, a second differential equation similar to the one described above is solved for the p side with appropriate boundary conditions. The solution to this equation is the current J_3. Because of light absorption in the p-region, the other two components just described become J_1' and J_2', and

$$J_{sc} = J_1 + J_2 = J_1' + J_2' + J_3. \tag{24}$$

For a given mobility, lifetime, barrier width, and thickness, the maximum short-circuit photocurrent J_{sc} is the same for Schottky barrier, p-n junction, and heterojunction devices. The short-circuit photocurrent as a function of thickness and diffusion length is shown in Fig. 10. The results shown here are for AMI spectrum with no losses due to reflection and electrode coverage. We have looked very critically in the region of very small diffusion length and found that the curves do not exactly extrapolate to zero as shown in Fig. 10. The short-circuit current as function of diffusion length below 1 μm is shown in Fig. 11. The initial fast rise is the result of light absorption in the barrier region. The results shown are for a barrier of 5000 Å wide.

These results indicate that even for a very small grain size of about 100 Å, a lifetime of about 5×10^{-11} sec, a barrier width of 5000 Å, and a 1 μm thick polycrystalline silicon film, one should still observe currents about 8 mA/cm^2 in AM1 spectrum. Obviously, if the barrier is narrower, then the current would decrease.

The diffusion length is related to the grain size by Eq. (11). Therefore, the short-circuit photocurrent can be expressed as a function of grain size d. Fig. 12 shows the variation of J_{sc} with the grain size d for different conditions. The experimental results are for a wide variety of devices fabricated under different conditions. Various light sources were used and the measurements vary from AM0 to AM2 conditions. Wherever possible, corrections are made to convert the result to AM1 conditions. We will show later that the thickness usually does not introduce large errors. The cell with a grain size of about 3 mm is a SnO_2/Si heterojunction cell fabricated in our laboratory (polysilicon obtained from Wacker).

Data below 10 μm grain sizes are due to Feldman, et al.[9] The polycrystalline silicon was deposited on glass or sapphire by electron beam evaporation of silicon. Junctions were then made by diffusion. Film thicknesses varied approximately between 2 and 30 μm and the device area was .06 mm^2. The light source was a 150 W xenon short arc lamp filtered by a 4 cm water path and a glass UV filter to produce an irradiance over the device of approximately 75 mW/cm^2 (AM2 sunlight). The data was corrected for electrode coverage but not for reflection. A single crystal monitor was used to compare the results. The short-circuit current they reported is the same as what we observe with our single crystal SnO_2/Si heterojunction solar cell in AM1 light with 10 percent reflection loss and 15 percent grid coverage.

Normally, J_{sc} values for AM1 are larger than AM2 but in this case we did not apply any correction. Further, for the mesa structure, errors are introduced due to diffusion from regions other than the mesa area.

For AM1 results, an increase of 20 percent in J_{sc} is assumed when no corrections are reported for reflection and electrode coverage, and for AM0 results no corrections were made. It is assumed for data taken in AM0 that the reduction in current due to conversion into AM1 irradiance is balanced out by the corrections necessary for reflection and electrode coverage. All of these will introduce an error between 10-15 percent for some devices. This may be small as compared to the uncertainty in the value of the grain size. In spite of these limitations, there is excellent agreement between theory and experiment. Comparing the theoretical curves with the experimental data one could conclude that in all probability there is barrier shrinkage when light is incident on polycrystalline silicon devices with grain sizes less than 10 μm, discussed below. The only other way the short-circuit current could be lower at smaller grain sizes were if the diffusion length was smaller than what we estimated. This implies either the lifetime or mobility was lower. Because of the close agreement between experimental and theoretical lifetime, we believe the only other alternative would be to have lower mobility than what we have assumed. We have also considered the mobility to change according to the following relation[38]

$$\mu_{eff} = \frac{n}{n+n_t}\,\mu \quad \text{for } d < 10\ \mu m \tag{25}$$

where n and n_t are the densities of free and trapped carriers, respectively. The results do not agree as well as those due to barrier shrinkage, as follows.

In modeling solar cells, the barrier is assumed to be constant, that is, having the same width in light and dark. For materials which are trap free and have long minority carrier diffusion lengths, this is a valid assumption. When light is incident, the shrinkage of the barrier with light is almost a universal phenomenon which has usually gone unnoticed due to the long diffusion length and its contribution to the current. It is observed even in single crystal material at high light intensities, but the shrinkage is small. However, the effect becomes pronounced in materials with traps which have low mobilities and lifetimes. We have observed the effect in organic materials,[39] in selenium,[40] and recently the effect has also been reported for amorphous silicon.[41] The effect is very similar to the narrowing of the barrier width with dopant concentration and the term "photon doping" well describes the phenomenon. Because of low mobilities and lifetimes, the barrier shrinkage has a large effect on the short-circuit photocurrent, and the device can no longer be considered as a constant current generator. However, the effect on the fill factor is estimated to be small.

Assuming that the barrier shrinks from 7500 Å to 500 Å for a grain size 10 μm or lower, the effect on short-circuit photocurrent is shown in Fig. 12. This is for a polycrystalline device 100 μm thick. In assuming a 500 Å barrier width, we are not saying that this is the actual width to be expected in light for all grain size below 10 μm. The results are presented just to show how the short-circuit current could decrease with decrease in barrier width as a result of trapping within the barrier region.

The last but not the least important factor which governs the short-circuit photocurrent is the thickness of the photoconductor, whether it be single crystal or polycrystalline. In Fig. 13 we show the variation of the short-circuit photocurrent as a function of grain size and thickness. As can be seen, the smaller the grain size, the lesser the effect of thickness. This is because the smaller the grain size, the smaller is the diffusion length, and an increase in thickness does not increase current because of the diffusion length limitation. These curves are important to calculations of the required grain sizes and thicknesses for a given efficiency. This will be evident later.

C. The Open-Circuit Photovoltage

The open-circuit photovoltage in polycrystalline silicon (as in single crystal) is given by the relation

$$V_{oc} \approx \frac{nkT}{q} \ln\left(\frac{J_{sc}}{J_o}\right). \tag{26}$$

For grain sizes 100 μm or lower, the recombination current is dominant, and as a result,

$$V_{oc} = \frac{2kT}{q} \ln\left(\frac{J_{sc}}{J_{or}}\right). \tag{27}$$

For d > 100 μm, the diffusion current is dominant and

$$V_{oc} = \frac{kT}{q} \ln\left(\frac{J_{sc}}{J_{od}}\right). \tag{28}$$

There may be a small transition range for MIS type devices where J_{ot} may influence V_{oc}.

The theoretical curves based on Eq. (27) and (28) are shown in Fig. 14. The results involve short-circuit photocurrent, with or without

barrier shrinkage, since the open-circuit photovoltage saturates at low current generation. There is excellent agreement between theory and experiment. Card and Yang's theory also agrees well with the experiment, but the agreement is accidental because they underestimated the magnitude of the short-circuit photocurrent. They only claimed an order of magnitude estimate. Other than Card and Yang, all other theoretical estimates of polycrystalline silicon only involve the short-circuit photocurrent.

D. Fill Factor

This is the first time calculation of the fill factor is ever computed as a function of grain size. The fill factor can be expressed as

$$F.F. = \left(1 - \frac{1}{\lambda V_{oc}}\right)\left(1 - \frac{\ln \lambda V_{oc}}{\lambda V_{oc}}\right) \qquad (29)$$

Since both λ and V_{oc} vary as a function of grain size, the F.F. is also expected to vary as function of grain size. Fig. 15 shows a plot of fill factor vs. grain size based on the theoretical V_{oc} vs. d plot in Fig. 14. There is excellent agreement between theory and experiment. The few deviations we feel are mainly due to series resistance effects. These results indicate that at small grain sizes the recombination process dominates the photovoltaic properties and overshadows the effect of series resistance on fill factor.

E. The Efficiency as a Function of Grain Size

Having calculated theoretically the short circuit photocurrent, the open-circuit photovoltage, and the fill factor, we are in a position to calculate the efficiency as a function of grain size. The result of such a calculation is shown in Fig. 16. The calculations are for a 100 μm thick device and involve both the curves for barrier shrinkage and no shrinkage.

For the experimental results, only the corrected values of short-circuit photocurrent in Fig. 12 are used. No corrections were used for the fill factor or the open circuit photovoltage. There is excellent agreement between experimental and theoretical values. The results indicate that one needs grain sizes greater than 100 μm for solar cells having efficiency of 10 percent or more.

F. Optimum Device Structure of Polycrystalline Silicon

To get the optimum device structure of polycrystalline silicon, the efficiency is plotted as a function of grain size for different thicknesses in Fig. 17. In Fig. 18 we have plotted thickness vs. grain size for 10 and 11 percent solar cells. The curves are similar to "phase diagrams" for thickness and grain size. It shows that for a 10 percent cell, we need grain sizes greater than 500 μm for 20 μm thick films. For thicknesses about 20 μm our predictions are in agreement with existing experimental data. The data of Chu[11] and D'Aiello et al.[13] supports the above conclusions.

IV. CONCLUSIONS

The grain size of silicon plays a dominant role in determining the electrical and photovoltaic properties of silicon. Grain boundaries act as traps and recombination centers. The recombination loss at grain boundaries is the predominant loss mechanism in polycrystalline solar cells. For small grain sizes, the surface recombination centers affect the lifetime more than any dopant concentration. One could fabricate 10 percent efficient polycrystalline silicon solar cells with 10 μm thick material if grain sizes were 5000 μm or greater. Excellent agreement is observed betwen theory and experiment for almost all device parameters. If lifetime and mobility values larger than those used in our calculation could be obtained, then the theoretical efficiency would be higher than what we have calculated. Though the present analysis was done for polycrystalline silicon, the qualitative features of the theory are applicable to any polycrystalline material. To obtain quantitative

data, some modification of our estimate of the cell parameters may be necessary, depending on the material. For materials with a direct band gap, smaller grain size and thicknesses are likely to result in efficiencies equivalent to thicker indirect band gap material of larger grain size. Furthermore, depending upon the height of the intergrain boundary barrier, tunnelling rather than thermionic emission may be the preferred mode of intergrain boundary crossing for carriers in the dark.

ACKNOWLEDGMENTS

The authors would like to thank Dr. H. Paul Maruska for many informative and stimulating discussions.

This work is supported in part by the U.S. Department of Energy, Division of Solar Energy under Contract No. DE-AC03-79ET23047.

REFERENCES

1. B. Authier, Patent #2508803 filed in the Federal Republic of Germany, September 9, 1976.
2. H. Fischer and W. Pschunder, 12th IEEE Photovoltaic Specialists Conference, p. 86 (1976).
3. J. W. Cleland, R. D. Westbrook, R. F. Wood and R. T. Young, Proc. of National Workshop on Low Cost Polycrystalline Silicon Solar Cell, p. 113 (1976).
4. K. R. Sarma, R. W. Gurther, A. Baghdadi, and M. Cota, Thin Films of Silicon on Low-Cost Substrate, Quarterly Report No. 4, Contract No. EY-76-C-03-1287 (unpublished).
5. M. Wolf, 11th IEEE Photovoltaic Specialist Conference p. 306, (1975).
6. T. L. Chu, 11th IEEE Photovoltaic Specialist Conference, p 303 (1975).
7. J. D. Zook, J. D. Heaps, R. B. Maciolek, B. Koepke, C. D. Butter, and S. B. Schuldt, Silicon on Ceramic Process, Annual Report No. 2, September 19, 1977, ERDA/JPL/954356-77/3 (unpublished).
8. C. Feldman, F. G. Satkiewicz, and H. K. Charles, Jr., Proc. of National Workshop on Low Cost Polycrystalline Silicon Solar Cell, p. 267 (1976).
9. C. Feldman, N. A. Blum, H. K. Charles, Jr. and F. G. Satkiewicz, J. of Electronic Materials. 7, 309 (1978).
10. J. Lindmayer, 12th IEEE Photovoltaic Specialist Conference, p. 82, (1976).
11. T. L. Chu, Semi-Annual Silicon Project In-Depth Review Meeting, May 4-5, 1978, Tycons Corner, Virginia (unpublished).
12. T. L. Chu, Applied Phys. Letters, 29, 675 (1976).
13. R.V. D'Aiello, ERDA/JPL 954817-78/13, Quarterly Report No. 2, April, 1978 (unpublished).

14. S. I. Soclof and P. A. Iles, 11th IEEE Photovoltaic Specialist Conference p. 56 (1975).

15. R. B. Hillborn, Jr., and T. Lin, Proc. of National Workshop on Low Cost Polycrystalline Solar Cell, p. 246 (1976).

16. C. Lanza and H. J. Hovel, 12th IEEE Photovoltaic Specialist Conference, p. 96 (1976).

17. H. C. Card and E. Yang, IEEE Transaction on Electron Devices, ED29, 397 (1977).

18. J. Y. W. Seto, J. Appl. Phys., 46, 5247 (1975).

19. M. E. Cowher and T. O. Sedgwick, J. Electrochem. Soc., 119, 1565 (1972).

20. A. L. Fripp and P. C. Arlotta, Proc. of National Workshop on Low Cost Polycrystalline Silicon Solar Cells, p. 59 (1976).

21. C. H. Seager and T. G. Castner, J. Appl. Phys., 49, 3879 (1978).

22. C. Baccarani, B. Ricco and G. Spadure, J. Appl. Phys., 49, 5565 (1978).

23. T. I. Kamins, J. Applied Phys., 42, 4357 (1971).

24. P. Rai-Choudhury and P. L. Hower, J. Electrochem. Soc., 120, 1761 (1975).

25. R. T. Young, J. W. Cleland and R. F. Wood, 12th IEEE Photovoltaic Conference, p. 65 (1976).

26. W. Shockley, Electrons and Holes in Semiconductors, pp. 318-325 (Wiley, New York, 1959).

27. J. J. Loferski, Proc. of Nat'l Workshop on Low Cost Polycrystalline Silicon Solar Cells, p. 308 (1976).

28. K. Y. Duh, S. S. Chu, T. L. Chu, and H. C. Mollenkopf, Proc. of Nat'l Workshop on Low Cost Polycrystalline Silicon Solar Cells, p. 255 (1976).

29. J. Manolu and T. I. Kamins, Solid-St. Electron, 15, 1103 (1972).

30. A. S. Grove, Physics and Technology of Semiconductor Devices, p. 187, (Wiley, New York, 1967).

31. T. L. Chu, Applied Phys. Letters 30, p. 425 (1977).

32. J. Shewchun, J. Dubow, A. Myszkowski and R. Singh, J. Appl. Phys. 49, 855 (1978).

33. A. K. Ghosh, C. Fishman and T. Feng, J. Appl. Phys., 49, 3490 (1978).

34. A. K. Ghosh, C. Fishman and T. Feng, J. of Appl. Phys. 50, 3454 (1979).

35. A. G. Milnes and D. L. Feucht, Heterojunctions and Metal Semiconductor Junctions, (Academic Press, New York, 1972).

36. H. J. Hovel Semiconductors and Semimetals, Vol. 11 Solar Cells (Academic Press, New York, 1975).

37. T. L. Chu, 12th IEEE Photovoltaic Specialist Conference, p. 76, (1976).

38. R. H. Bube, Photoconductivity of Solids, p. 69 (John Wiley, New York, 1967).

39. A. K. Ghosh and T. Feng, J. Appl. Phys., 49, 5982 (1978).

40. R. F. Shaw and A. K. Ghosh, U.S. Pat. #4064 522 Dec. 20, 1977 and associated unpublished results.

41. C. R. Wronski, IEEE Trans. on Electron Devices, ED24, p. 351 (1977).

FIGURE CAPTIONS

Fig. 1 Efficiency vs. grain size. The curves are theoretical results, and the data points are experimental values obtained by different research groups. O-Feldman et al. (Ref. 9); ▲-Chu et al. (Refs. 6,11); Δ-Fischer and Pschunder (Ref. 2); □-Zook et al (Ref. 7).

Fig. 2 Grain boundaries at different physical locations within a solar cell.

Fig. 3 Average free carrier concentration and mobility as a function of doping density in polycrystalline silicon. The mobilities are for majority carriers. The grain sizes of the n-type and p-type silicon are 25 μm (Ref. 25) and 200-270Å (Ref. 18), respectively. The straight line is the carrier concentration vs. doping concentration for single crystal.

Fig. 4 Mobility-minimum doping density vs. grain size. The experimental data were taken from Refs. 18, 19, 23 and 25.

Fig. 5 Resistivity vs. doping concentration of polycrystalline silicon as compared with single crystal results. The grain sizes of the n-type and p-type silicon are 25 μm (Ref. 25) and 200-270Å (Ref. 18), respectively.

Fig. 6 Mobility vs. grain size. O-electron mobility for n-type polycrystalline silicon. ▲-hole mobility for p-type polycrystalline silicon. ■-mobility for electron and hole. □-average minority carrier mobility for single crystal silicon. The experimental values were obtained from Refs. 18,19, 23, and 25.

Fig. 7 Lifetime vs. grain size. The experimental data were taken from Refs. 9,28,29, and 30. The lifetime from Ref. 9 was estimated.

Fig. 8 Diffusion length as a function of grain size. The theoretical curves I and II are for no changes in mobility and for changes in mobility according to Fig. 6, respectively. O-from Ref. 9 ▲-from Ref. 31.

Fig. 9 Reverse saturation current J_{or} (due to recombination) as a function of grain size. The W for the two theoretical curves are barrier widths. O-Feldman et al. (Refs. 8,9); ▲-Chu et al. (Ref. 11,37); ●-Hovel (Ref. 36).

Fig. 10 Short-circuit photocurrent vs. diffusion length. t is the thickness of the film. AMI irradiance.

Fig. 11 Short-circuit photocurrent vs. diffusion length. AM1 irradiance.

Fig. 12 Effect of barrier shrinkage and mobility on J_{sc}. Experimental data were taken from Refs. 2,6,7,9,11 and present work. ●-Present work; all other symbols are the same as in Fig. 1. Where appropriate, corrections have been made for reflection and grid coverage losses. All data shown were normalized to AM1 spectrum.

Fig. 13 Effect of thickness on short-circuit photocurrent. t is the thickness of the film.

Fig. 14 Effect of grain size on V_{oc}. The theoretical curve I is obtained by assuming barrier shrinkage, and curve II assumes no shrinkage. Experimental data were taken from Refs. 2,6,7,9,11 and present work.

Fig. 15 Effect of grain size on fill factor. The theoretical curve I is obtained by assuming barrier shrinkage, and curve II assumes no shrinkage. Experimental data were taken from Refs. 2,7,7,9,11, and present work.

Fig. 16 Effect of grain size on efficiency with (I) and without (II) barrier shrinkage. Experimental data were from Refs. 2,6,7,9,11, and present work.

Fig. 17 Effect of grain size on efficiency at different thicknesses t.

Fig. 18 Grain size and thickness relationship for 10 and 11% efficiency cells.

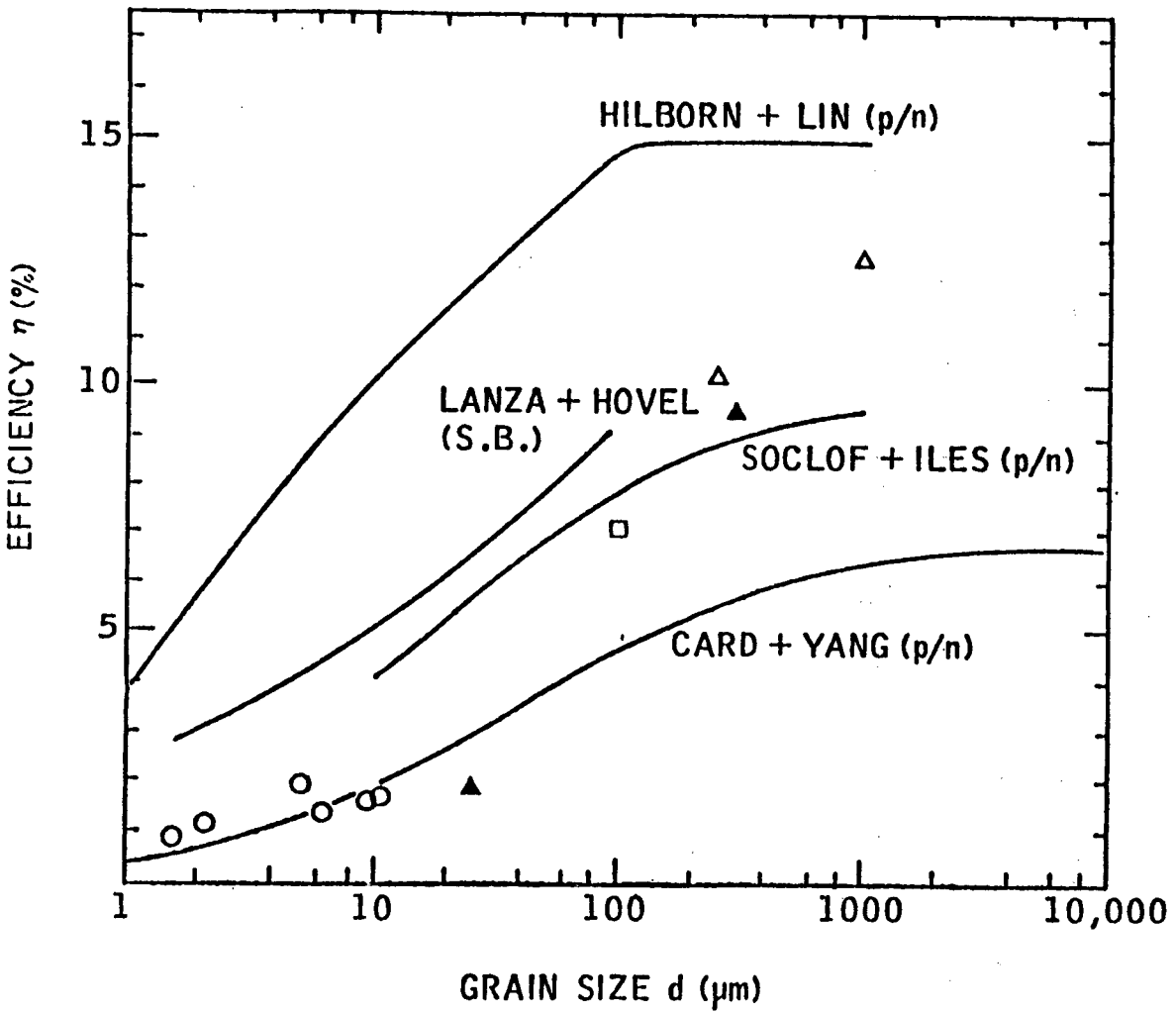
HILBORN + LIN (p/n)
LANZA + HOVEL
(S.B.)
SOCLOF + ILES (p/n)
CARD + YANG (p/n)
EFFICIENCY η (%)
15
10
5
1
10
100
1000
10,000
GRAIN SIZE d (μm)

FIGURE 1

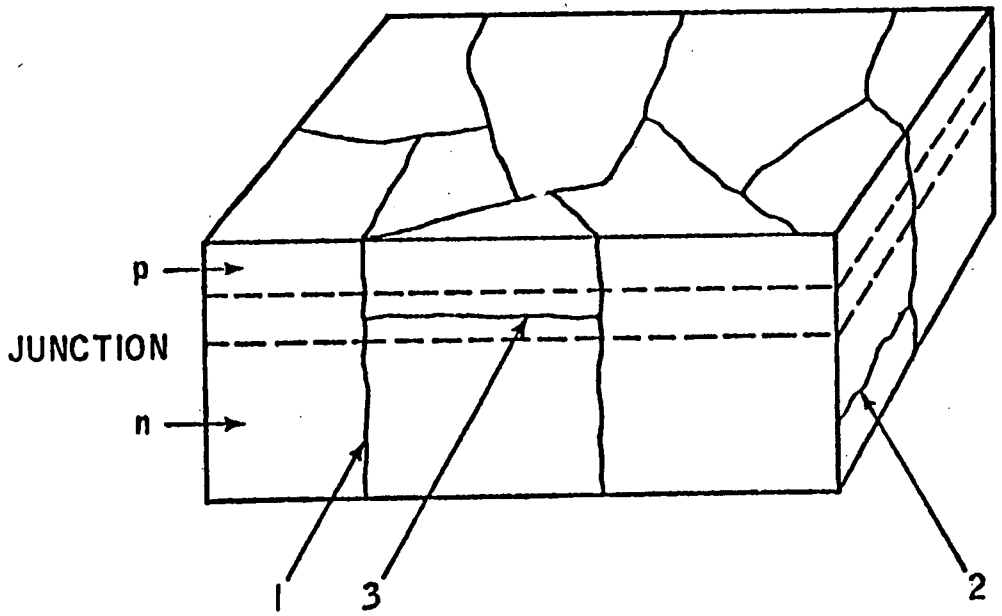

FIGURE 2

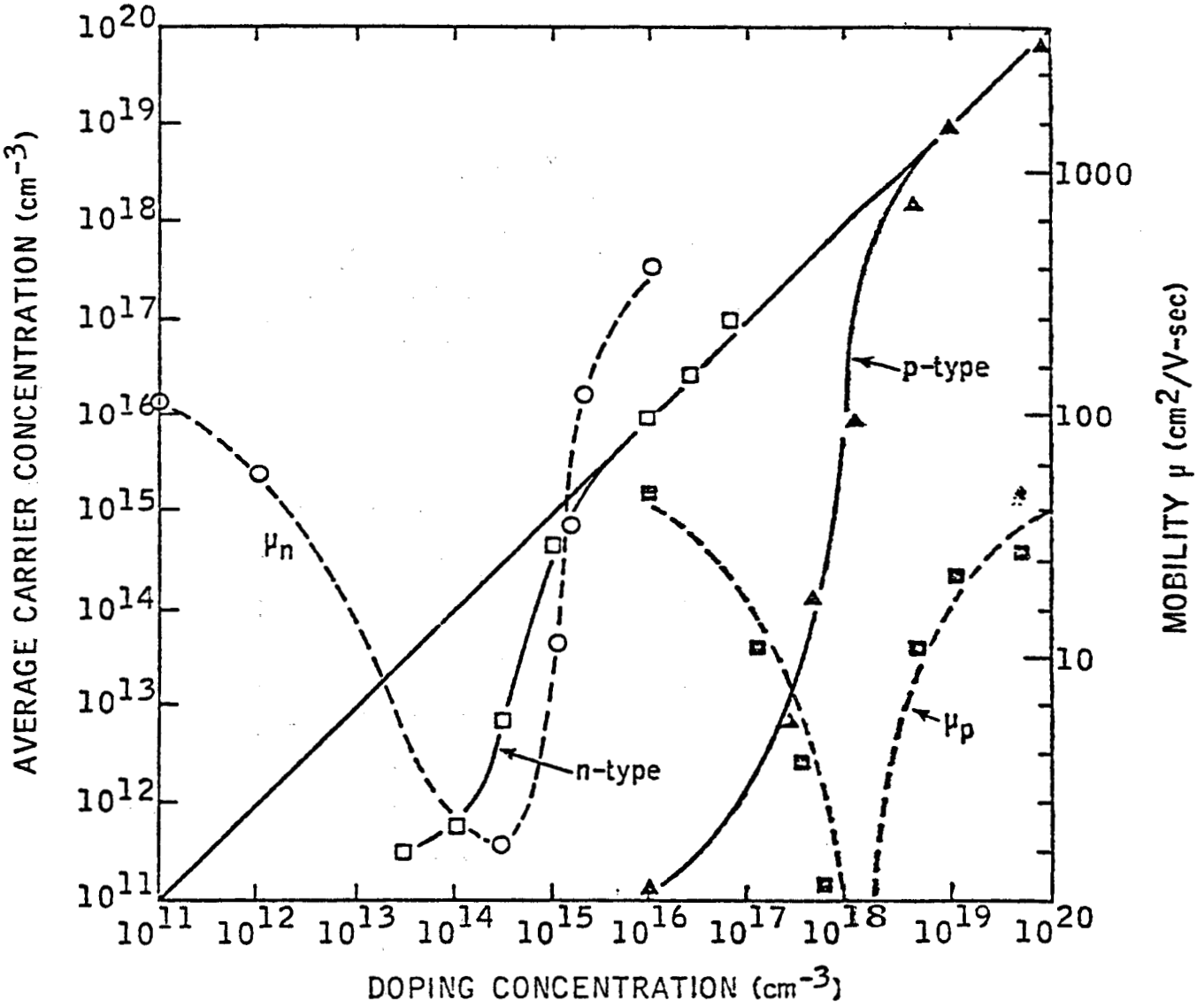
AVERAGE CARRIER CONCENTRATION (cm^{-3})
MOBILITY μ (cm^2/V-sec)
DOPING CONCENTRATION (cm^{-3})
10^{20}
10^{19}
10^{18}
10^{17}
10^{16}
10^{15}
10^{14}
10^{13}
10^{12}
10^{11}
1000
100
10
10^{11} 10^{12} 10^{13} 10^{14} 10^{15} 10^{16} 10^{17} 10^{18} 10^{19} 10^{20}
μ_n
μ_p
n-type
p-type

FIGURE 3

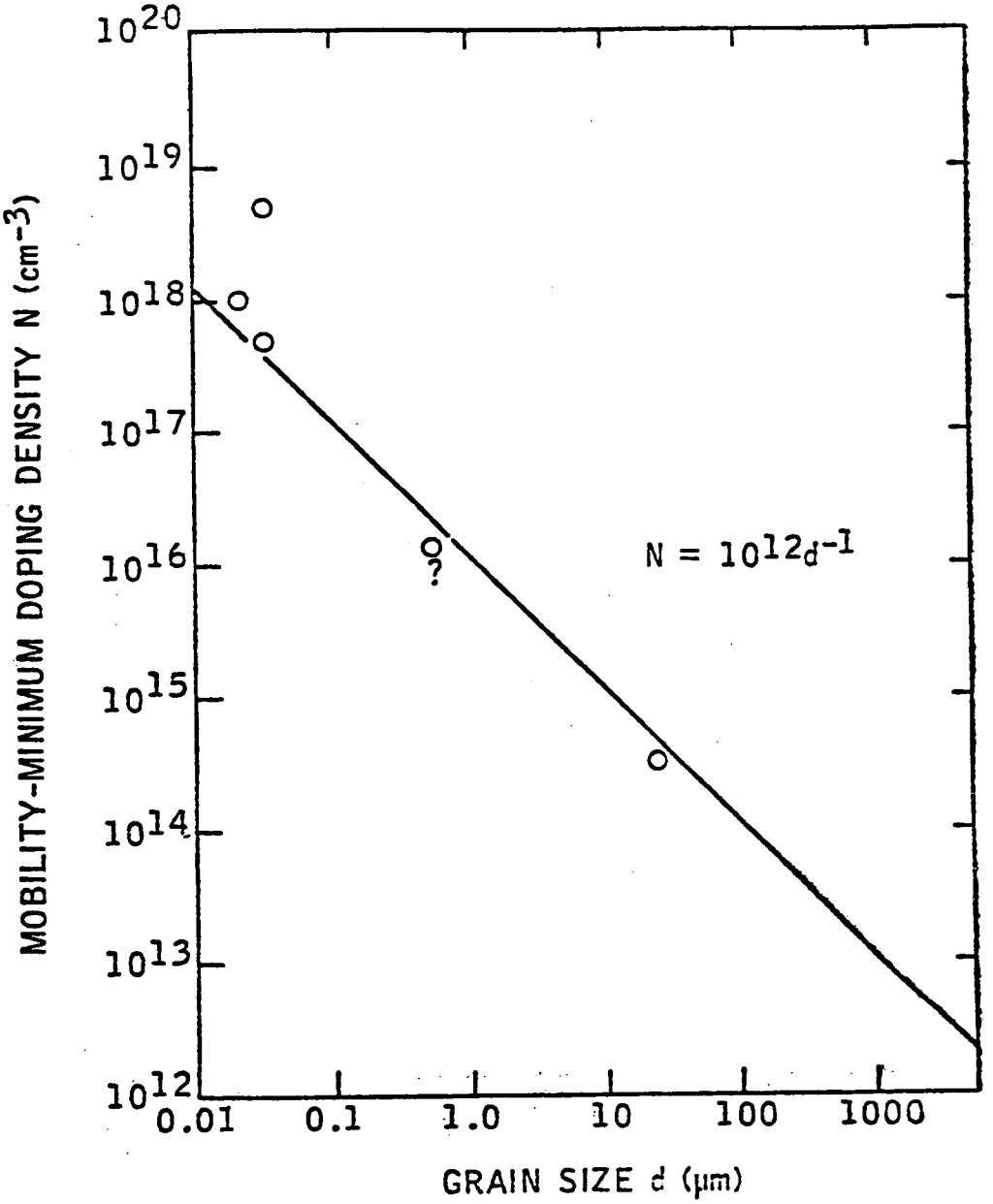
MOBILITY-MINIMUM DOPING DENSITY N (cm^{-3})
10^{20}
10^{19}
10^{18}
10^{17}
10^{16}
10^{15}
10^{14}
10^{13}
10^{12}
0.01
0.1
1.0
10
100
1000
GRAIN SIZE d (μm)
N = $10^{12}d^{-1}$
?

FIGURE 4

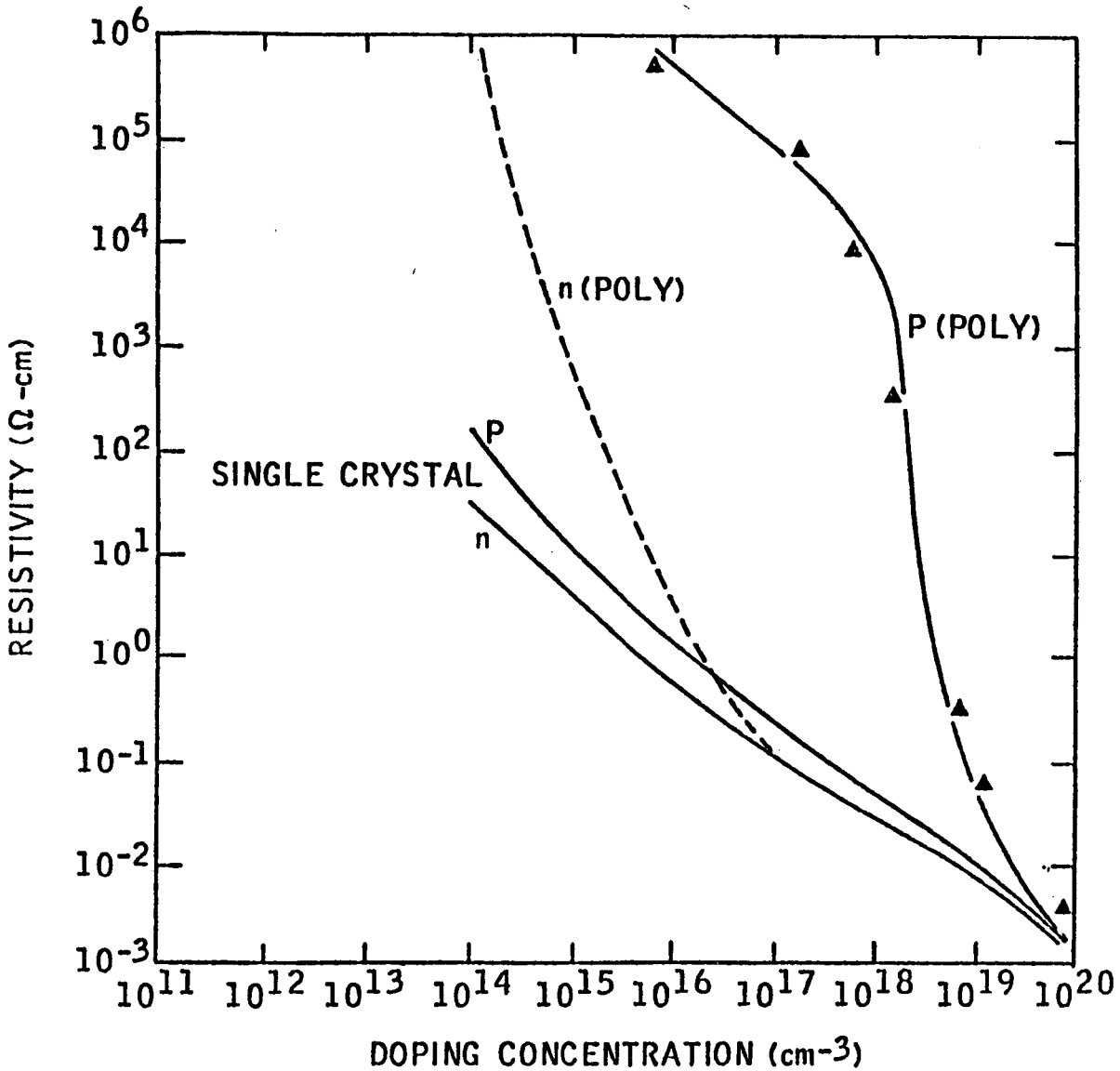
RESISTIVITY (Ω-cm)
10^6
10^5
10^4
10^3
10^2
10^1
10^0
10^{-1}
10^{-2}
10^{-3}
n (POLY)
P (POLY)
P
SINGLE CRYSTAL
n
10^{11} 10^{12} 10^{13} 10^{14} 10^{15} 10^{16} 10^{17} 10^{18} 10^{19} 10^{20}
DOPING CONCENTRATION (cm-3)

FIGURE 5

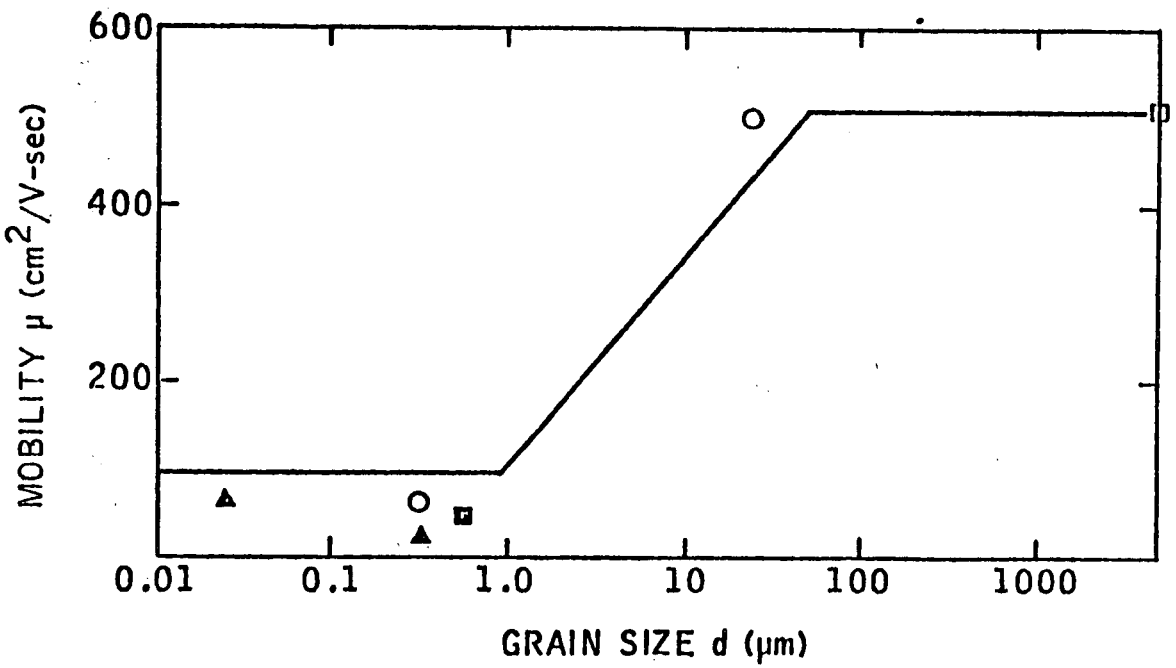
600
400
200
MOBILITY μ (cm²/V-sec)
0.01
0.1
1.0
10
100
1000
GRAIN SIZE d (μm)

FIGURE 6

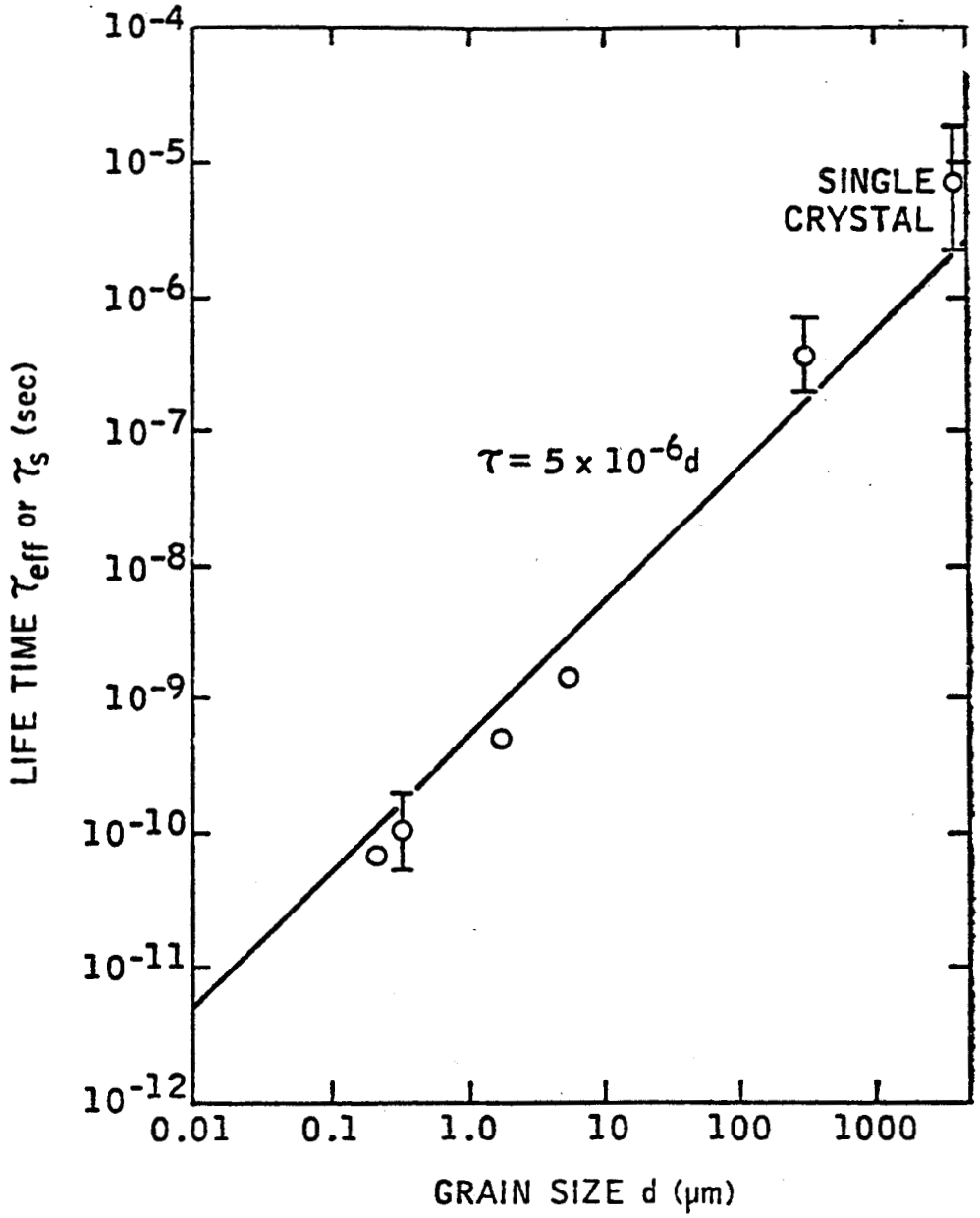
LIFE TIME τ_{eff} or τ_s (sec)
10^{-4}
10^{-5}
10^{-6}
10^{-7}
10^{-8}
10^{-9}
10^{-10}
10^{-11}
10^{-12}
SINGLE CRYSTAL
$\tau = 5 \times 10^{-6} d$
0.01
0.1
1.0
10
100
1000
GRAIN SIZE d (μm)

FIGURE 7

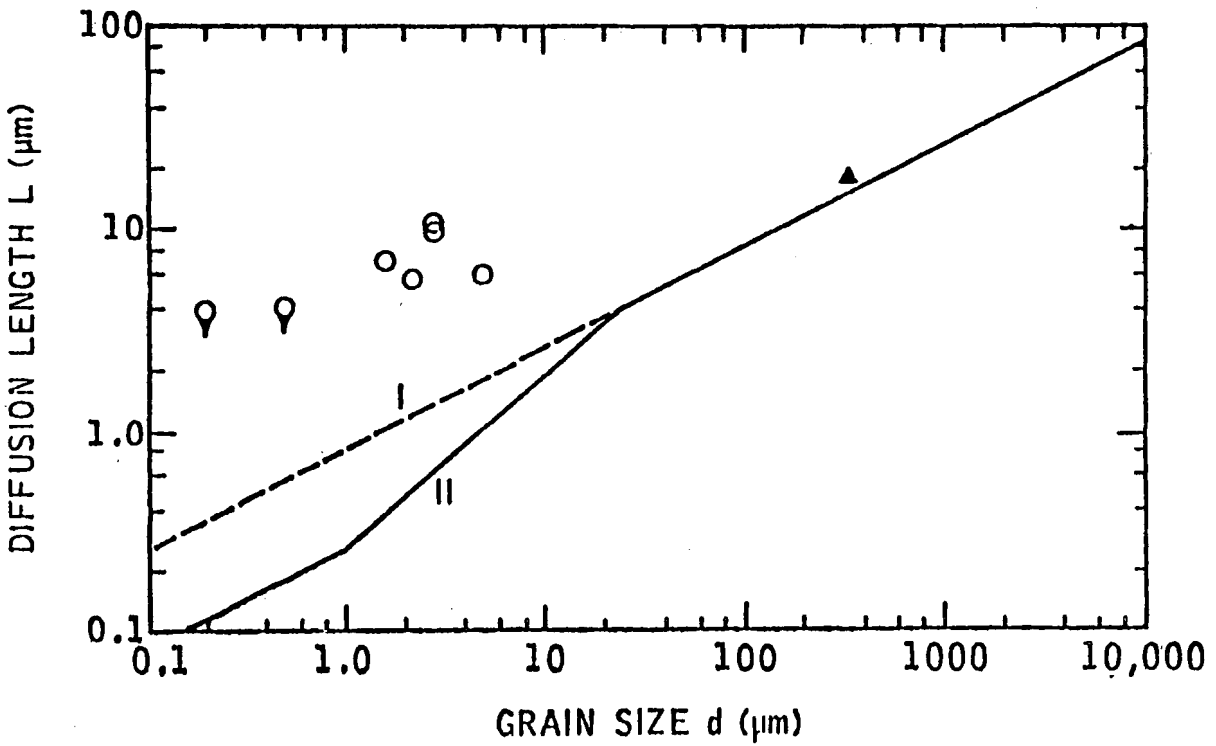
100
10
1.0
0.1
DIFFUSION LENGTH L (μm)
0.1
1.0
10
100
1000
10,000
GRAIN SIZE d (μm)
I
II

FIGURE 8

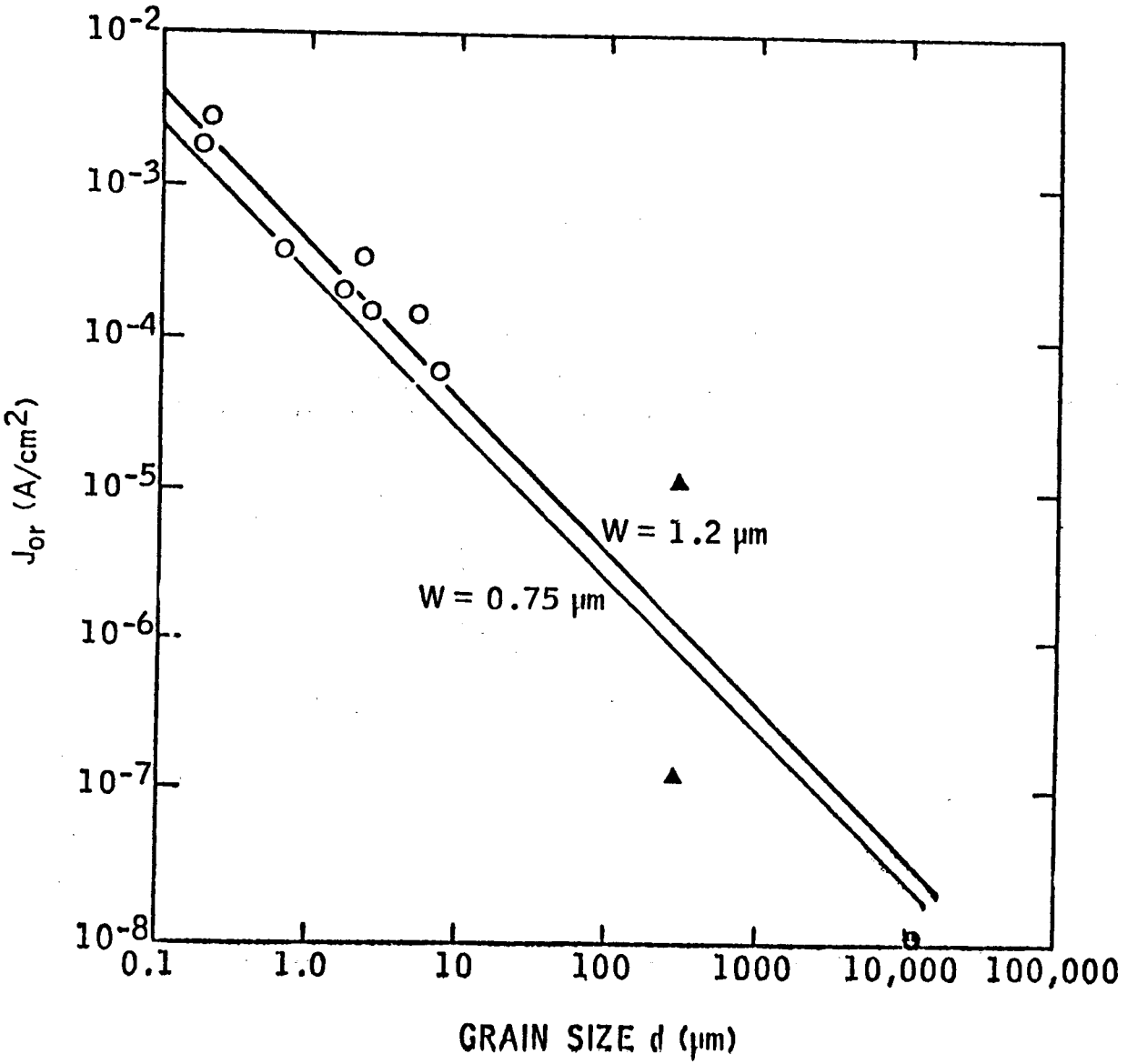
10^{-2}
10^{-3}
10^{-4}
10^{-5}
10^{-6}
10^{-7}
10^{-8}
J_{or} (A/cm^2)
W = 1.2 μm
W = 0.75 μm
0.1
1.0
10
100
1000
10,000
100,000
GRAIN SIZE d (μm)

FIGURE 9

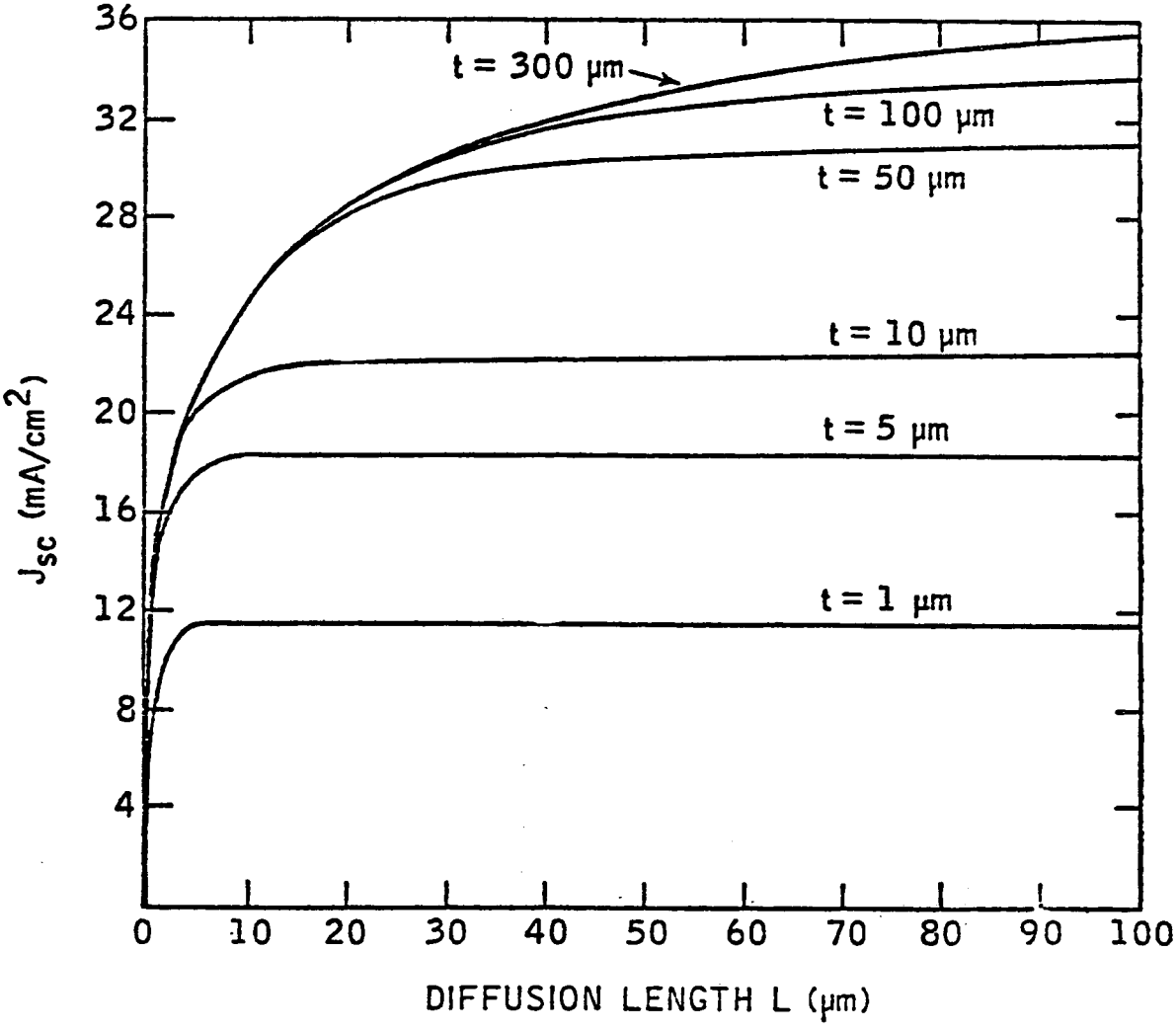
36
32
28
24
20
16
12
8
4
J_{sc} (mA/cm^2)
t = 300 μm
t = 100 μm
t = 50 μm
t = 10 μm
t = 5 μm
t = 1 μm
0
10
20
30
40
50
60
70
80
90
100
DIFFUSION LENGTH L (μm)

FIGURE 10

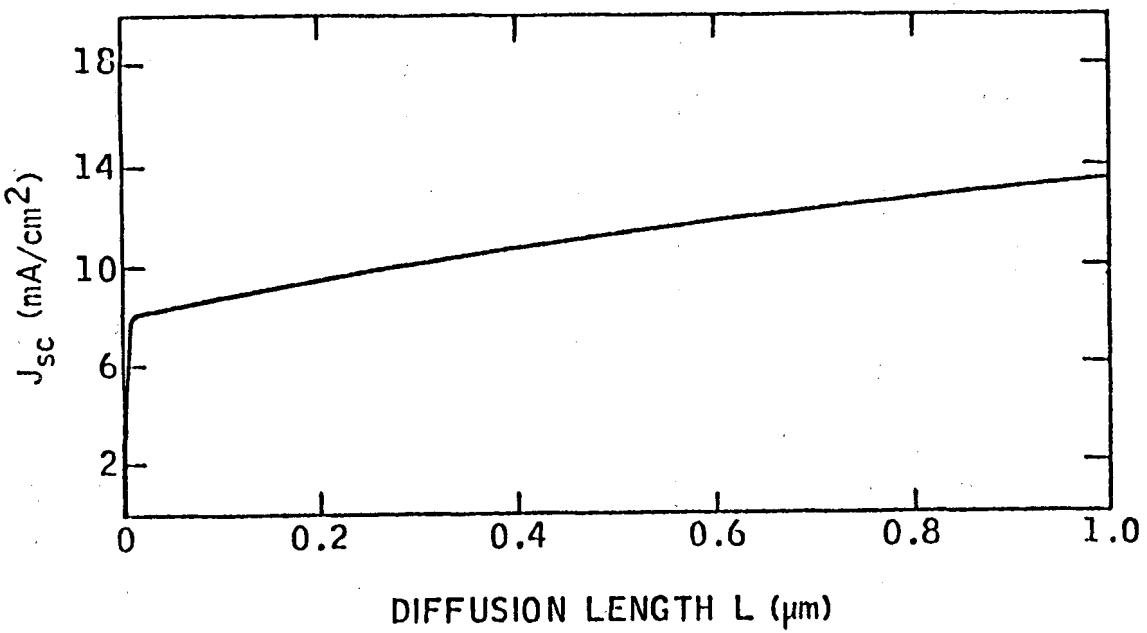

FIGURE 11

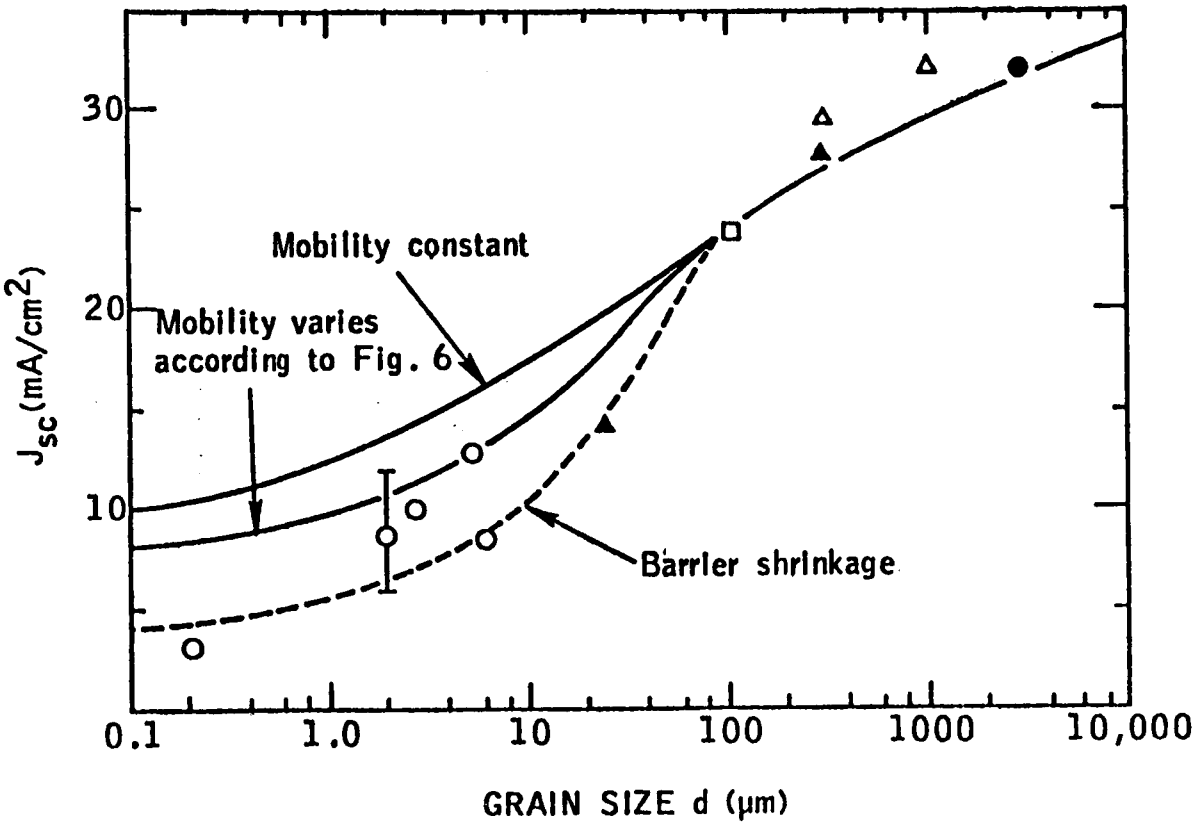
30
20
10
J_{sc}(mA/cm^2)
Mobility constant
Mobility varies
according to Fig. 6
Barrier shrinkage
0.1
1.0
10
100
1000
10,000
GRAIN SIZE d (μm)

FIGURE 12

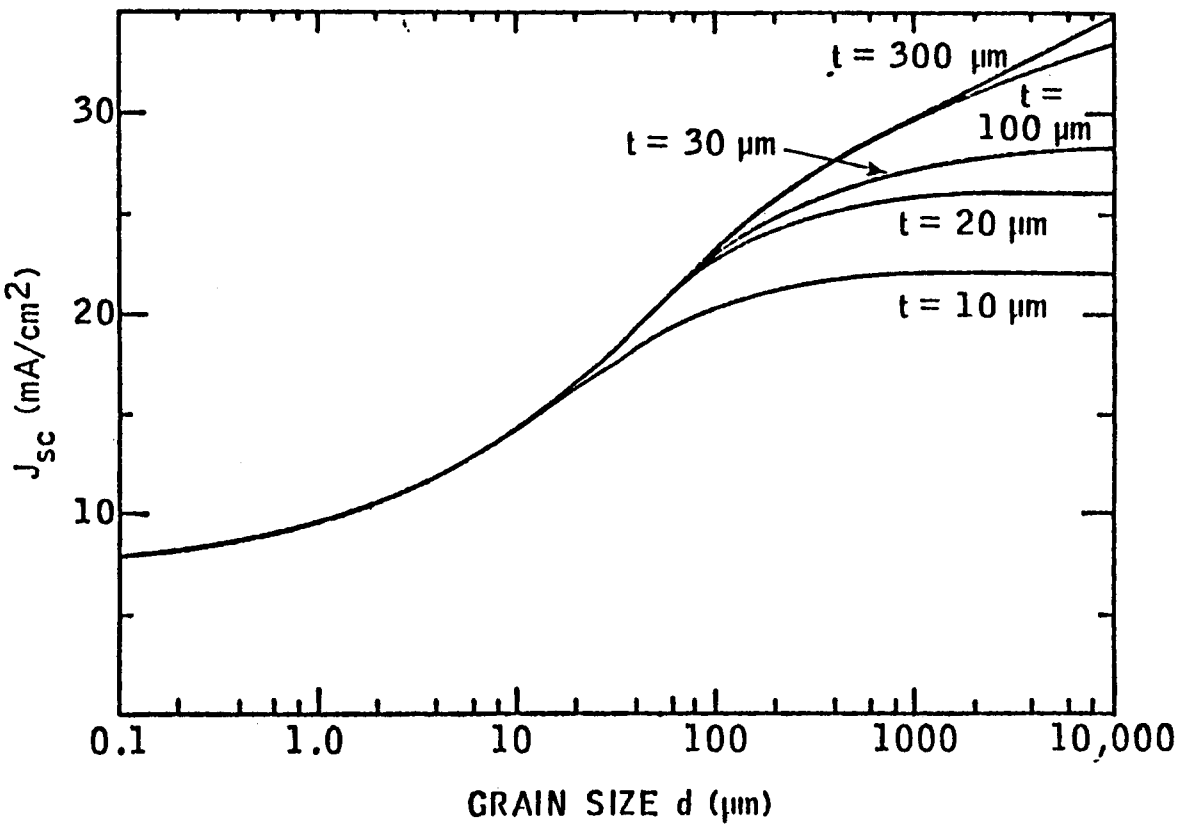
t = 300 µm
t = 100 µm
t = 30 µm
t = 20 µm
t = 10 µm
30
20
10
J_{sc} (mA/cm^2)
0.1
1.0
10
100
1000
10,000
GRAIN SIZE d (µm)

FIGURE 13

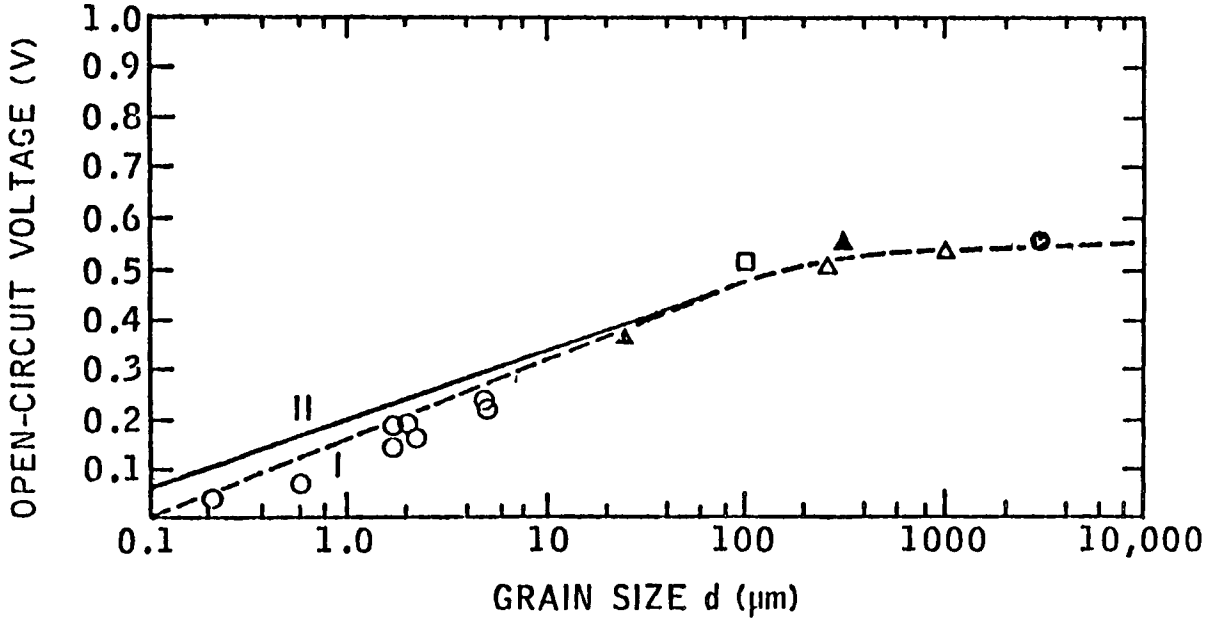
OPEN-CIRCUIT VOLTAGE (V)
1.0
0.9
0.8
0.7
0.6
0.5
0.4
0.3
0.2
0.1
0.1
1.0
10
100
1000
10,000
GRAIN SIZE d (μm)

FIGURE 14

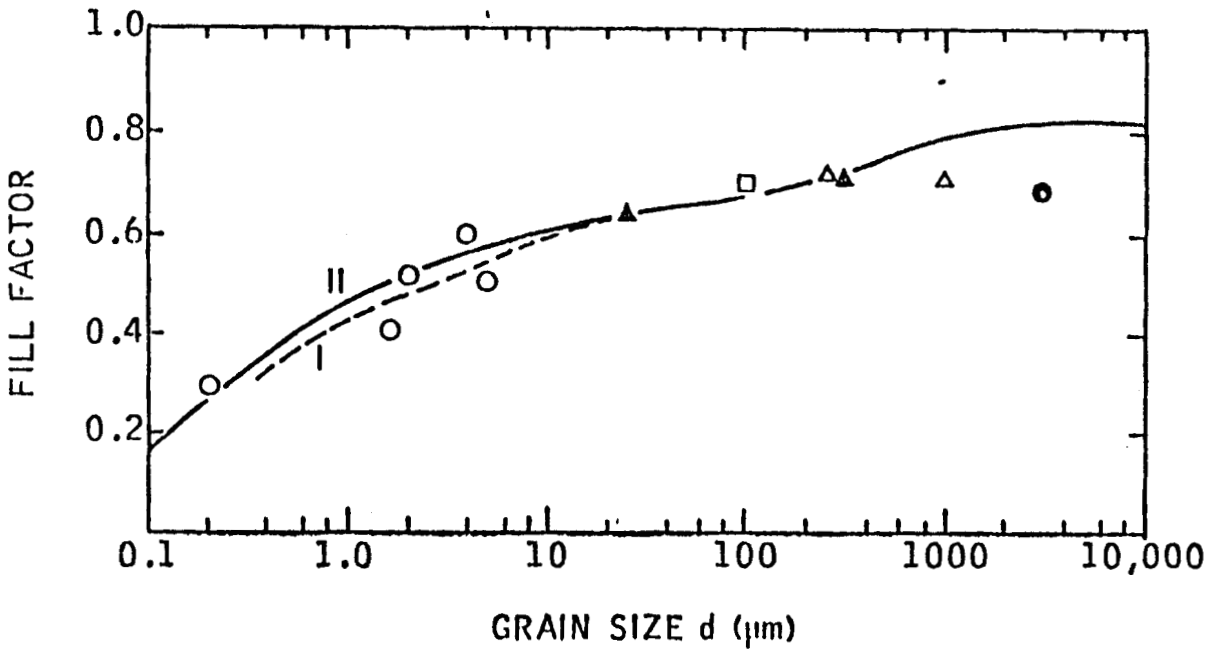
1.0
0.8
0.6
0.4
0.2
FILL FACTOR
0.1
1.0
10
100
1000
10,000
GRAIN SIZE d (μm)
II
I

FIGURE 15

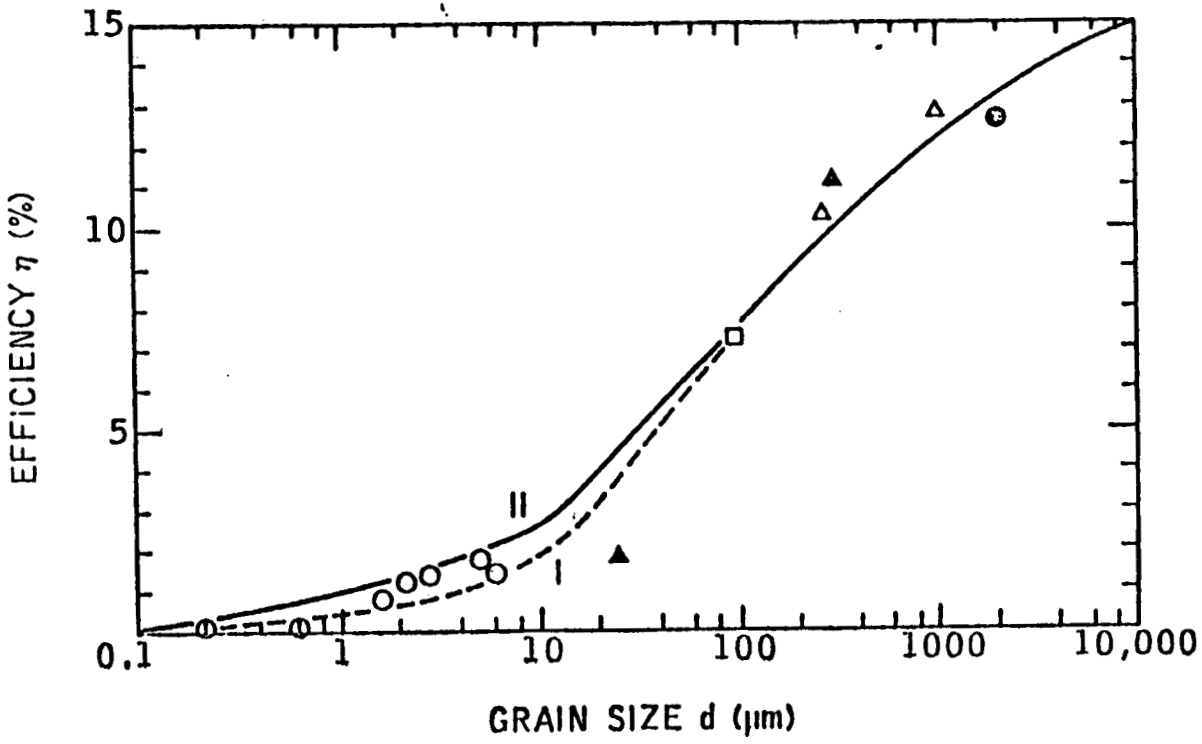

FIGURE 16

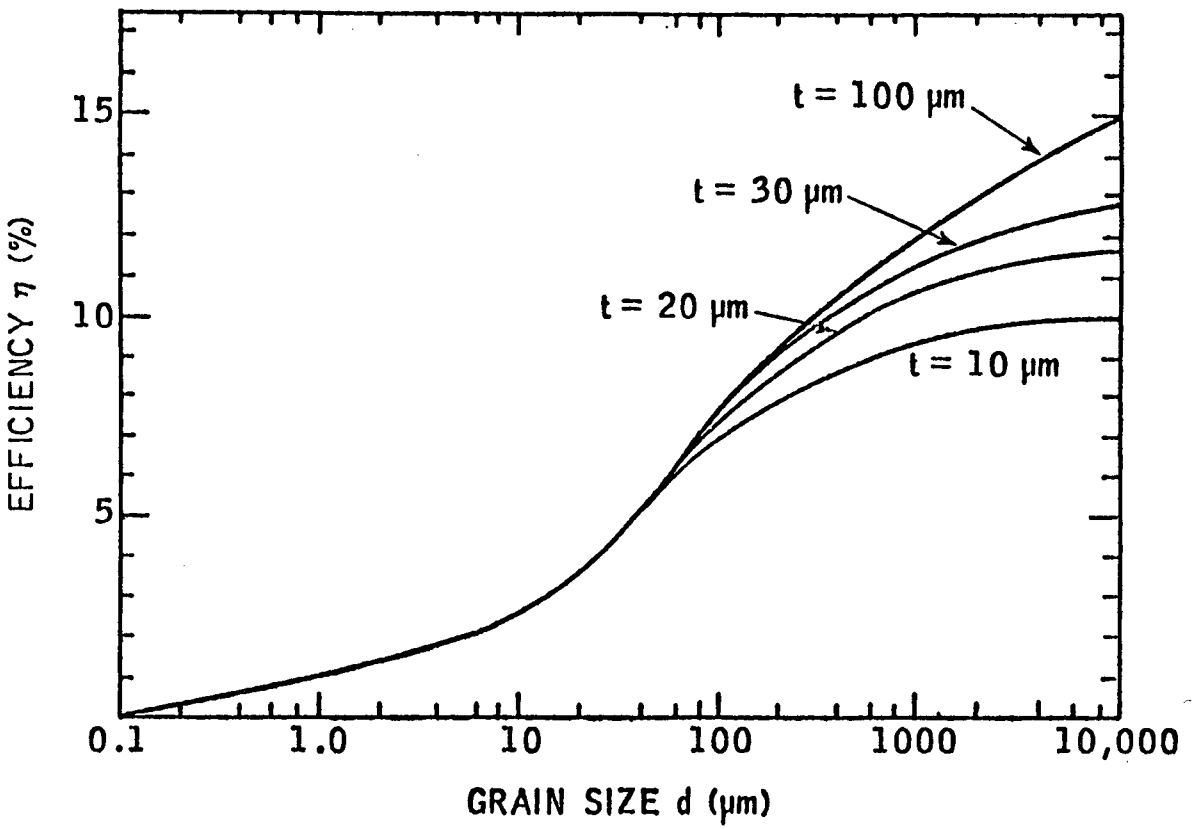
t = 100 μm
t = 30 μm
t = 20 μm
t = 10 μm
15
10
5
EFFICIENCY η (%)
0.1
1.0
10
100
1000
10,000
GRAIN SIZE d (μm)

FIGURE 17

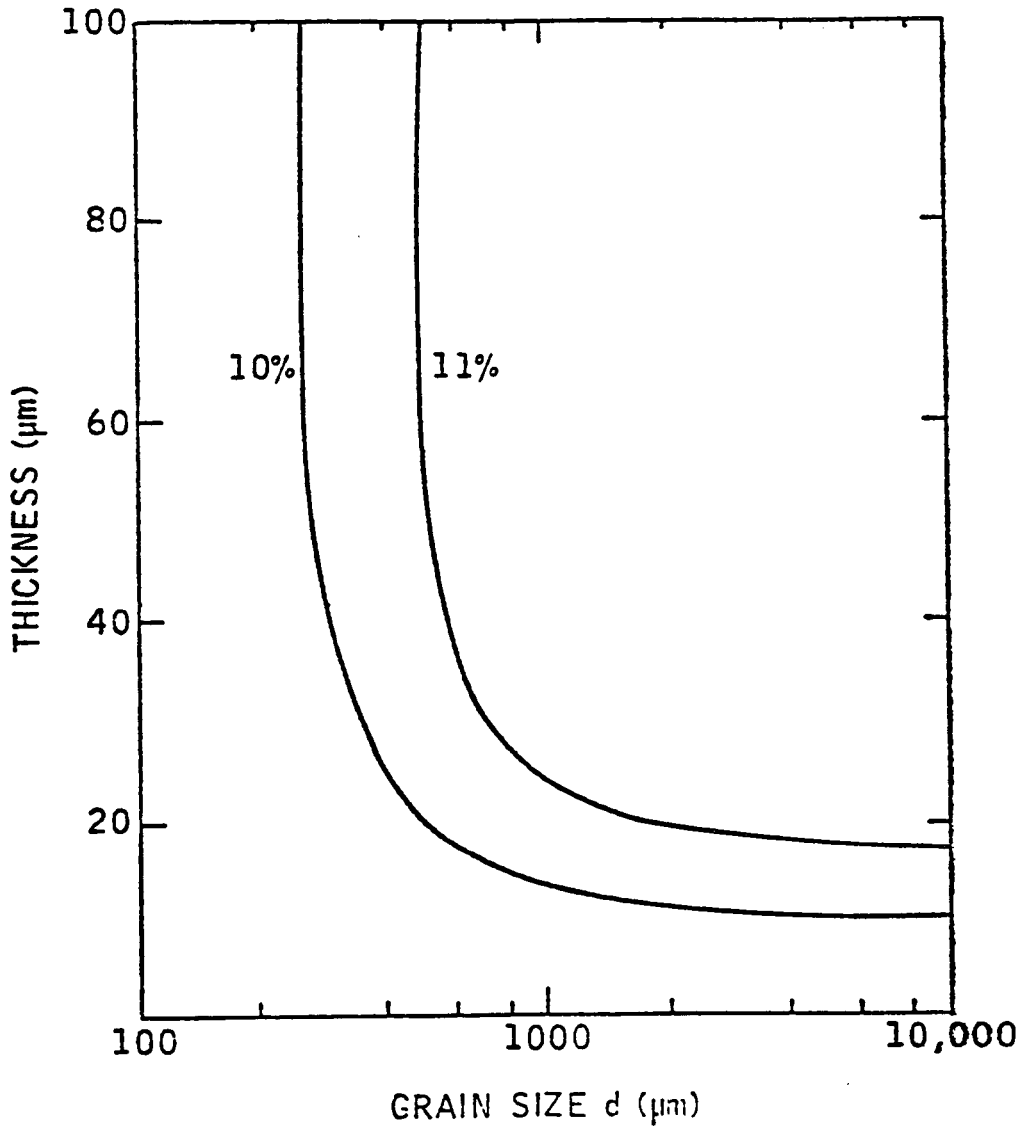

FIGURE 18

☆U.S. GOVERNMENT PRINTING OFFICE: 1980-640-258-1779